Controls on leaf water hydrogen and oxygen isotopes: A local investigation across seasons and altitude

Jinzhao Liu[a, b*], Chong Jiang[a], Huawu Wu[c], Li Guo[d], Haiwei Zhang[e]

[a] State Key Laboratory of Loess and Quaternary Geology, Institute of Earth Environment, Chinese Academy of Sciences, Xi'an 710061, China

[b] National Observation and Research Station of Earth Critical Zone on the Loess Plateau of Shaanxi, Xi'an, 710061, China

[c] Key Laboratory of Watershed Geographic Sciences, Nanjing Institute of Geography and Limnology, Chinese Academy of Sciences, Nanjing 210008, China

[d] State Key Laboratory of Hydraulics and Mountain River Engineering & College of Water Resource and Hydropower, Sichuan University, 610065, Chengdu, China

[e] Institute of Global Environmental Change, Xi'an Jiaotong University, Xi'an, 710054, China

*Corresponding author's email: liujinzhao@ieecas.cn (J. Liu)

Abstract

The stable oxygen ($\delta^{18}O_{leaf}$) and hydrogen ($\delta^{2}H_{leaf}$) isotopes of leaf water act as a bridge that connects hydroclimate to plant-derived organic matter. However, it remains unclear whether the source water (i.e., twig water, soil water, and precipitation) or meteorological parameters (i.e., temperature, relative humidity, and precipitation) are the dominant controls on $\delta^{18}O_{leaf}$ and $\delta^{2}H_{leaf}$. Here, we reported seasonal analysis of $\delta^{18}O_{leaf}$ and $\delta^{2}H_{leaf}$ together with isotopes from potential source waters and meteorological parameters along an elevation transect on the Chinese Loess Plateau. We found that $\delta^{2}H_{leaf}$ values were more closely correlated with source water isotopes than $\delta^{18}O_{leaf}$ values, whereas $\delta^{18}O_{leaf}$ and $\delta^{2}H_{leaf}$ values were similarly correlated with meteorological parameters. Dual-isotope analysis showed that the $\delta^{18}O_{leaf}$ and $\delta^{2}H_{leaf}$ values were closely associated because of their similar altitudinal and seasonal responses, generating a well-defined isotope line relative to the local meteoric water line (LMWL). We also compared the measured $\delta^{18}O_{leaf}$ and $\delta^{2}H_{leaf}$ values with predicted values by the Craig-Gordon model, and found no significant differences between them. We demonstrate that the first-order control on $\delta^{18}O_{leaf}$ and $\delta^{2}H_{leaf}$ values was the source water, and the second-order control was the enrichment associated with biochemical and environmental factors.

Short Summary

What controls leaf water isotopes? We answered the question from two perspectives: respective and dual isotopes. On the one hand, the $\delta^{18}O$ and $\delta^{2}H$ values of leaf water responded to isotopes of potential source water (i.e., twig water, soil water, and precipitation) and meteorological parameters (i.e., temperature, RH, and precipitation) differently. On the other hand, dual $\delta^{18}O$ and $\delta^{2}H$ values of leaf water yielded a significant regression line, associated with altitude and seasonality.

Keywords: Leaf water, stable isotope, controls, seasonality, altitude

1 Introduction

The stable isotope compositions of oxygen and hydrogen ($\delta^{18}O$ and $\delta^{2}H$, respectively) are increasingly being used as powerful tracers to follow the path of water from its input as precipitation, movement through the soil, and ultimately to its release as soil evaporation and leaf transpiration (Penna and Meerveld, 2019). Leaf water transpiration plays a key role in regulating water balance at scales ranging from catchment to global. Terrestrial plants can enrich heavier isotopes (^{2}H and ^{18}O) in leaf water via evaporative fractionation through the stoma (Helliker and Ehleinger, 2000; Liu et al., 2015; Cernusak et al., 2016), which is highly dependent on atmospheric conditions (e.g., temperature and relative humidity) and biophysiological processes (Farquhar et al., 2007; Kahmen et al., 2011; Cernusak et al., 2016). Subsequently, the isotopic signals from the leaf water are integrated into plant organic matter, such as cellulose (e.g., Barbour, 2007; Lehman et al., 2017) and leaf wax (Liu et al., 2016, 2021), as powerful proxies used for paleoclimate reconstruction (Pagani et al., 2006; Schefuβ et al., 2011; Hepp et al., 2020). However, although leaf water isotopes are the fundamental parameters in ecohydrology and organic biosynthesis, we still lack an adequate understanding of what controls leaf water isotopes, or the role of source water and hydroclimate in influencing leaf water isotopes?

$\delta^{18}O_{leaf}$ and $\delta^{2}H_{leaf}$ values are influenced firstly by a plant's source water (mainly water taken up by roots from the soil; Cernusak et al., 2016; Barbour et al., 2017; Munksgaard et al., 2017), and secondly by the enrichment associated with transpiration (Munksgaard et al., 2017). Soil water for terrestrial plants generally originates from local precipitation, and precipitation isotopes vary spatially and temporally, being subject to controls including temperature, altitude, latitude, distance from the coast, and amount of precipitation (Bowen, 2010; Bowen and Good, 2015; Cernusak et al., 2016). More specifically, soil water isotopes are determined by a mixture of individual precipitation events with distinct isotopic signals and are also affected by evaporation, both of which lead to the development of isotopic gradients in soil water with depth (Allison et al., 1983; Liu et al., 2015). A number of studies have shown that the $\delta^{18}O$ and $\delta^{2}H$ values of root/xylem water can be used to characterize the water sources used by plants (Rothfuss and Javaux, 2017; Wu et al., 2018; Wang et al., 2019; Amin et al., 2020; Zhao et al., 2020; Liu et al., 2021a). These studies rested substantially on the assumption that no isotopic fractionation of $\delta^{18}O$ and $\delta^{2}H$ values occur during water uptake by plant roots (Dawson and Ehleringer, 1991; Ehleringer and Dawson, 1992; Chen et al., 2020), except in saline or xeric environments (Lin and Sternberg, 1993; Ellsworth and Williams, 2007). Some recent studies have shown, however, that the occurrence of isotopic fractionation during root water uptake was probably more common than previously thought, especially with respect to $\delta^{2}H$ values (Zhao et al., 2016; Wang et al., 2017; Barbeta et al., 2019; Poca et al., 2019; Liu et al., 2021a).

In addition to plant source water, leaf water is also isotopically enriched through the evaporative process of transpiration. The enrichment of ^{18}O and ^{2}H by leaf water transpiration can be predicted using the Craig-Gordon model (C-G model). This model was initially proposed to describe the evaporative enrichment of a freely evaporating water body (Craig and Gordon, 1965) and has been modified for plant leaves under steady-state conditions (Dongmann et al., 1974; Farquhar and Cernusak, 2005). However, the C-G model fails to explain the intra-leaf heterogeneity of $\delta^{18}O_{leaf}$ and $\delta^{2}H_{leaf}$ (Cernusak et al., 2016; Liu et al., 2021b), which is currently described using a two-pool model (Leaney et al., 1985; Song et al., 2015) and/or an advection-diffusion model, as the *Péclet* effect (Farquhar and Lloyd, 1993; Farquhar and Gan, 2003). Subsequently, more complicated models have been developed to cover non-steady-state conditions (Ogée et al., 2007). These models emphasize a mechanistic understanding of leaf water isotopic fractionation, but the relevant parameters cannot be strictly constrained or precisely monitored, which hinders the use of these models under natural conditions (Plavcová et al., 2018).

This study combined the effects of measured source water isotopes and C-G model-predicted transpiration on $\delta^{18}O_{leaf}$ and $\delta^{2}H_{leaf}$ values. Our objectives were to deepen the understanding of the controls on the $\delta^{18}O_{leaf}$ and $\delta^{2}H_{leaf}$ values, and explore the seasonal variations of these controls. Based upon these objectives, we repeatedly sampled soils, twigs, and leaves in May, July, and September (representing spring, summer, and autumn, respectively) from the same ten plots distributed along an elevation transect. Simultaneously, we obtained the relevant meteorological parameters (e.g., temperature, relative humidity, and precipitation) from sites close to the sampling plots along the transect and used these to predict the $\delta^{18}O_{leaf}$ and $\delta^{2}H_{leaf}$ values. The combined analysis of concurrent measurements of $\delta^{18}O$ and $\delta^{2}H$ values in soil water, twig water, and leaf water with the predicted $\delta^{18}O$ and $\delta^{2}H$ values of leaf water from the C-G model associated with the surrounding meteorological parameters will help to identify the factors that control $\delta^{18}O_{leaf}$ and $\delta^{2}H_{leaf}$ values. Furthermore, we performed an isotope-based line analysis of the dual $\delta^{18}O$ and $\delta^{2}H$ values of leaf water, associated with altitude and seasonality. This study will improve our understanding of the environmental signals preserved within the $\delta^{18}O$ and $\delta^{2}H$ values extracted from plant organic biomarkers associated with leaf water.

2. Materials and Methods

2.1 Study area

The Qinling Mountains form the dividing line between northern and southern China and mark the boundary between the watersheds of the Yellow and Yangtze rivers. Mt. Taibai (Fig. 1; 33. 96 °N, 107.77 °E) rises to 3767 m above sea level (asl) and is the peak in the Qinling Mountains; it has a warm temperate ecosystem characterized by a rich diversity of flora and fauna. The mean annual temperature at the bottom of Mt. Taibai is 12.9°C, and mean annual precipitation is 609.5 mm (Zhang and Liu, 2010). The climate, soil, and vegetation vary significantly along our slope transect, exhibiting a remarkable vertical geo-ecological zonation (Fig. 1). The area contains a variety of climate zones: warm temperate (< 1300 m asl), temperate (1300 - 2600 m asl), cool temperate (2600 - 3350 m asl), and alpine (> 3350 m asl). The soil types vary from yellow loess soil at low elevations, spectacular rocky outcrops at middle elevations, and glacial remnants at high elevations. Vegetation along the transect is mainly coniferous and broadleaf forests and alpine and subalpine vegetation (Fig. 1; Liu, 2021). The dominant species range from *Quercus variabilis*, *Q. aliena*, *Betula albosinensis*, *B. utilis*, *Abies fargessi,* and *Larix chinensis* forests to *Rhododendron clementinae* and *R. concinnum* alpine (Supplementary table S1).

2.2 Sampling strategy

Plants and soils were sampled in May, July, and September 2020, and samples were collected from 10 plots (3 × 3 m) covering all of the vegetation zones along the northern slope of Mt. Taibai, extending from 608 to 3533 m asl (Fig. 1). Among the plots, six sites (i.e., site 2, 3, 4, 5, 8, 10; Fig. 1) were selected as being the closest to the weather stations along the elevation transect, and they were used order to obtain the *in-situ* meteorological data for analysis. For the plants, one or two dominant deciduous and coniferous trees were chosen in each plot across the vegetation zone (Supplementary Table S1). Several large leaves and suberized twigs were collected for each species. Three to ten large leaves were chosen for sampling, and a small number were collected in broadleaf forests and a large number in coniferous forests, depending on leaf size. The leaf samples were conducted in the context of the intact leaves because of the likely isotopic gradients within a leaf (Helliker and Ehleringer, 2000; Liu et al., 2016). Our sampling period was between 12 pm and 3 pm because maximum diurnal enrichment of the leaf water isotopic composition occurs during this part of the day

(Romero and Feakins, 2011; Liu et al., 2021). The twigs were collected simultaneously by cutting suberized twigs, and all of the twigs were cut into samples that were 3-4 cm long. The leaf and twig samples were immediately placed into glass vials with screw caps and sealed with polyethylene parafilm. For the soils, three surface soil samples (less than 10 cm deep) were collected from around the sampled plants using a small metal scoop at each plot. All sampling plots were located on slopes far from rivers and surface water bodies, which ensured that the soil water in each plot was derived exclusively from precipitation. Although the surface soil layers were collected only as the representative of soil water in this study, these samples could provide a relatively good source of water for the plants, as supported by a prior study conducted along the same elevation transect (Zhang and Liu, 2010). The soil samples were tightly sealed in a polyethylene zipper bag on site. All plant and soil samples were stored in a cool box (~ 4 °C) in the field and immediately transported to the laboratory. The altitude of each plot was determined using a handheld GPS unit with an error of ± 5 m.

2.3 Isotope analysis

The water in the plant and soil samples was extracted using an automatic cryogenic vacuum extraction system (LI-2100 Pro, LICA United Technology Limited, Beijing, China). The auto-extraction process was set for 3 hours, and the extraction rate of water from samples was more than 98%. The isotopic composition of soil water was measured using a Picarro L2130-I isotope water analyzer (Sunnyvale, CA, USA) at the State Key Laboratory of Loess and Quaternary Geology, Institute of Earth Environment, Chinese Academy of Sciences. The analytical accuracies were ±0.1‰ for $\delta^{18}O$ and ±1‰ for

δ^2H. The isotopic measurements of twig and leaf water were conducted using an isotope ratio mass spectrometer coupled to a high-temperature conversion elemental analyzer (HT2000 EA-IRMS, Delta V Advantage; Thermo Fisher Scientific, Inc. USA) at the Huake Precision Stable Isotope Laboratory on the campus of Tsinghua Shenzhen International Graduate School. The measurement precisions were ± 0.2‰ and ± 1‰ for $\delta^{18}O$ and δ^2H, respectively. The isotopic composition of $\delta^{18}O$ and δ^2H is expressed as an isotopic ratio:

$$\delta_{sample}(‰) = \left(\frac{R_{sample} - R_{standard}}{R_{standard}}\right) \times 1000 \qquad (1)$$

where δ_{sample} represents $\delta^{18}O$ or δ^2H, and R_{sample} and $R_{standard}$ indicate the ratio of $^{18}O/^{16}O$ or $^2H/^1H$ of the sample and standard, respectively. The $\delta^{18}O$ and δ^2H values are reported relative to the Vienna mean standard ocean water (VSMOW). In addition, the mean monthly $\delta^{18}O$ and δ^2H values of precipitation were determined using the Online Isotope in Precipitation Calculator (Bowen and Revenaugh, 2003).

2.4 Modeling isotopes of leaf water

The C-G equation can be approximated as (Cernusak et al., 2022),

$$\delta_e = \delta_s + \varepsilon^+ + \varepsilon_k + (\delta_v - \delta_s - \varepsilon_k) \times \frac{e_a}{e_i} \qquad (2)$$

where δ_e is the predicted $\delta^{18}O$ and δ^2H values at the evaporative sites within leaves, δ_s is the $\delta^{18}O$ and δ^2H values of source water (equivalent to twig water in our study), ε^+ is the equilibrium fractionation between liquid water and vapour, and ε_k is the kinetic fractionation during the diffusion of vapour through the stomata and the boundary layer.

In our analysis, we calculated Δ_v (the enrichment of atmospheric vapour relative to source water) as $\Delta_v = (\delta_v - \delta_s)/(1+\delta_s)$, and the values of Δ_v is often close to $-\varepsilon^+$ at the isotopic steady state (Barbour, 2007; Cernusak et al., 2016); therefore we can calculate δ_v as $\delta_v = -\varepsilon^+ + (1-\varepsilon^+)\delta_s$. In addition, $\frac{e_a}{e_i}$ is the ratio of the water vapour pressure fraction in the air relative to that in the intercellular spaces and is equal to the relative humidity (RH) in the air at the steady state (Cernusak et al., 2022). Thus, Equation (2) can be derived as,

$$\delta_e = (1-h)(\varepsilon^+ + \varepsilon_k) + (1-\varepsilon^+ h)\delta_s \qquad (3)$$

where δ_s represents the isotopic values of twig water, and h is the mean annual or monthly RH (MARH or MMRH) in this study. The equilibrium fractionation (ε^+) varies as a function of temperature (Bottinga and Craig, 1969), and can be equated to $\delta^{18}O$ and $\delta^{2}H$, as follows (Majoube, 1971):

$$\varepsilon_O^+(‰) = \left[\exp\left(\frac{1.137}{(273+T)^2}\times 10^3 - \frac{0.4156}{273+T} - 2.0667\times 10^{-3}\right) - 1\right]\times 1000 \qquad (4)$$

$$\varepsilon_H^+(‰) = \left[\exp\left(\frac{24.844}{(273+T)^2}\times 10^3 - \frac{76.248}{273+T} + 52.612\times 10^{-3}\right) - 1\right]\times 1000 \qquad (5)$$

The kinetic fractionation (ε_k) can be calculated for $\delta^{18}O$ and $\delta^{2}H$ as (Farquhar et al., 2007; Cernusak et al., 2016):

$$\varepsilon_k^O(‰) = \frac{28r_s+19r_b}{r_s+r_b} \qquad (6)$$

$$\varepsilon_k^H(‰) = \frac{25r_s+17r_b}{r_s+r_b} \qquad (7)$$

where r_s and r_b are the resistances of the stomatal and boundary layers, respectively, and the inverse of the conductance of the stomatal and boundary layers, respectively. Previous studies found stomatal and boundary layer conductance values of 0.49 and 2.85 mol m^{-2} s^{-1}, respectively (Cernusak et al., 2016; Munksgaard et al., 2017), resulting in ε_k^O and ε_k^H values of 26.7 and 23.8, respectively.

2.5 Statistical analysis

Statistical analysis (i.e., the mean, maximum and minimum values, as well as the standard deviation) of the isotopes extracted from the precipitation, soil, twig, and leaf samples was performed to define the range and distribution of the $\delta^{18}O$ and $\delta^{2}H$ values across the seasons. The Pearson correlation method was used to assess the correlations between the $\delta^{18}O$ and $\delta^{2}H$ values among the different water types (i.e., precipitation, soil water, twig water, and leaf water). Hierarchical cluster analysis was used to show the relationships among $\delta^{18}O_{leaf}$ and $\delta^{2}H_{leaf}$ values and potential source water isotopes ($\delta^{18}O$ and $\delta^{2}H$ values in precipitation, soil water, twig water, and leaf water), and meteorological parameters such as mean annual and monthly precipitation (MAP and MMP), mean annual and monthly temperature (MAT and MMT), and mean annual and monthly relative humidity (MARH and MMRH). A one-way analysis of variance (ANOVA) combined with a *post hoc* Tukey's least significant difference (LSD) test was performed to identify the significant differences in the isotopic compositions of precipitation, soil, twig, and leaf waters across the months. Comparisons of the relationships of $\delta^{18}O$ and $\delta^{2}H$ in the soil and leaf water were performed using covariance analysis (ANCOVA) to compare slopes across months. The structural equation model (SEM) was used to explain the respective effects of source waters (i.e., twig water, soil water, and precipitation) and meteorological parameters (i.e., temperature, precipitation, and RH) on $\delta^{18}O_{leaf}$ and $\delta^{2}H_{leaf}$ values. The validated SEMs generated a good model fit, as indicated by a non-significant χ^2 test ($p > 0.05$), a high comparative fit index (CFI > 0.95), and a low root mean square error of approximation

(RMSEA < 0.05). A special SEM was constructed based on the Mantel R values in AMOS (version 24.0.0). Moreover, we used the Hybrid Single-Particle Lagrangian Integrated Trajectory (HYSPLIT) model (Draxler and Rolph, 2003) to calculate air mass back-trajectory for a central site (34.13°N, 107.83°E, 2270 m asl) in the study area. These trajectories were initiated four times daily (at 00:00, 06:00, 12:00, and 18:00 UTC), and their air parcel was released at 2300 m asl for May, July, and September 2020 and moved backward by winds for 120 h (5 days).

3. Results

3.1 Differing response of $\delta^{18}O$ and $\delta^{2}H$ values of leaf water

The measured $\delta^{18}O$ and $\delta^{2}H$ values of leaf water responded differently to source water isotopes (Fig. 2a) and meteorological parameters (Fig. 2b) across the seasons. Cluster analysis showed that the leaf water $\delta^{18}O$ and $\delta^{2}H$ values ($\delta^{18}O_{leaf}$ and $\delta^{2}H_{leaf}$) were clustered with the twig water $\delta^{18}O$ and $\delta^{2}H$ values ($\delta^{18}O_{twig}$ and $\delta^{2}H_{twig}$; Fig. 2a), and also with MARH, MAT, and MMT (Fig. 2b). The $\delta^{2}H_{leaf}$ values were more closely correlated with isotopes of the potential source waters (e.g., twig water, soil water, and precipitation) than the $\delta^{18}O_{leaf}$ values in different months (Fig. 2a). In contrast, leaf water $\delta^{18}O$ and $\delta^{2}H$ values were correlated with meteorological parameters (Fig. 2b) across months. These correlations were more significant in summer (July) and autumn (September) than those in spring (May).

3.2 Comparisons of measured and predicted $\delta^{18}O$ and $\delta^{2}H$ values of leaf water

The $\delta^{18}O_{leaf}$ and δ^2H_{leaf} values predicted by the C-G model were compared with the measured $\delta^{18}O$ and δ^2H values across all three months (Fig. 3). The C-G models explained 49% and 70% of the observed variations in the $\delta^{18}O_{leaf}$ and δ^2H_{leaf} values, respectively (Fig. 3a, c). The slopes of the relationships for both $\delta^{18}O$ and δ^2H values of leaf water were less than one, which suggests that part of the bulk leaf water is derived from unenriched vein water. However, there were no significant differences in $\delta^{18}O_{leaf}$ ($p = 0.54$; Fig. 3b) and δ^2H_{leaf} values ($p = 0.93$; Fig. 3d) between the C-G model predicted values and the measured values.

3.3 Variation of $\delta^{18}O$ and δ^2H values of different waters with seasons and altitude

There was a significant correlation between $\delta^{18}O_{leaf}$ and δ^2H_{leaf} values ($R^2 = 0.81$, $p < 0.01$; Fig. 4), with significant clusters of $\delta^{18}O_{leaf}$ and δ^2H_{leaf} values across the months, and values being higher in May, intermediate in July, and lower in September (Fig. 4). Within each month, the $\delta^{18}O_{leaf}$ and δ^2H_{leaf} values were depleted in ^2H and ^{18}O at higher altitudes relative to lower altitudes. Likewise, the potential types of source water (i.e., twig water, soil water, and precipitation) exhibited consistent variations across the months, showing values that were relatively higher in May, intermediate in July, and lower in September (Supplementary Fig. S1). The correlations between $\delta^{18}O$ and δ^2H values among the source waters were also significant (Supplementary Fig. S2). Still, the slopes and coefficients of determination (R^2) between the $\delta^{18}O$ and δ^2H values showed decreasing trends for precipitation, soil water, twig water, and leaf water from the three sampling months, except for soil water in May (Supplementary Fig. S2). In addition, the ANCOVA tests showed no significant differences for the regression lines for precipitation (df = 0.47, $F = 2.49$, $p = 0.11 > 0.05$), twig water (df = 53.2, $F = 0.42$, $p = 0.66 > 0.05$), and leaf water (df = 437.3, $F = 2.78$, $p = 0.08 > 0.05$) across the months, but a significant difference for soil water across the months (df = 308.8, $F = 10.9$, $p < 0.05$).

4. Discussion

4.1 $\delta^{18}O$ and $\delta^{2}H$ values of leaf water

A recent global meta-analysis indicated that $\delta^{18}O_{leaf}$ and $\delta^{2}H_{leaf}$ values reflect environmental drivers differently and showed that $\delta^{2}H_{leaf}$ values more strongly reflect xylem water and atmospheric vapour $\delta^{2}H$ values, whereas $\delta^{18}O_{leaf}$ values more strongly reflect air relative humidity (Cernusak et al., 2022). Seasonal and localized observations along an elevation transect on the Chinese Loess Plateau supported these differred responses of $\delta^{18}O_{leaf}$ and $\delta^{2}H_{leaf}$ to isotopic composition of the potential source water and meteorological parameters (Fig. 2). This is likely due to the range of variation in precipitation isotopic values compared with that in leaf water evaporative enrichment is larger for $\delta^{2}H_{leaf}$ than $\delta^{18}O_{leaf}$ (Cernusak et al., 2022). In addition, we found stronger correlations between $\delta^{2}H_{leaf}$ and isotope values of the source water (twig water, soil water, and precipitation) than between $\delta^{18}O_{leaf}$ values and the source water isotope values (Fig. 2a). This is consistent with the global meta-analysis (Cernusak et al., 2022). However, our localized observational study did not show a significantly different response of $\delta^{18}O_{leaf}$ and $\delta^{2}H_{leaf}$ values to meteorological parameters, which responded at an almost equivalent magnitude (Fig. 2b). These observations suggest that plant organic isotopic proxies such as leaf wax (Sachse et al., 2012; Liu et al., 2016) and cellulose (Barbour, 2007; Lehman et al., 2017), which originate from $\delta^{18}O_{leaf}$ and δ^2H_{leaf} values, can provide comparative information that indicates climatic signals (e.g., temperature, RH, and precipitation) in natural archives. These results argued with the recent global meta-analysis that $\delta^{18}O_{leaf}$ and δ^2H_{leaf} values reflect climatic parameters (i.e., RH and temperature) differently (Cernusak et al., 2022).

The results of the cluster analysis showed that the isotope values of leaf water ($\delta^{18}O_{leaf}$ and δ^2H_{leaf}) and twig water ($\delta^{18}O_{twig}$ and δ^2H_{twig}) were clustered into one group, but those of soil water ($\delta^{18}O_{soil}$ and δ^2H_{soil}) and precipitation ($\delta^{18}O_p$ and δ^2H_p) were clustered into another (Fig. 2a). This indicates that the direct source water of $\delta^{18}O_{leaf}$ and δ^2H_{leaf} should be $\delta^{18}O_{twig}$ and δ^2H_{twig}, providing the source water isotope basis for the C-G model. In the C-G model (see Equation 2), besides the source water isotopes, the equilibrium fractionation factor (ε^+) and atmospheric vapour enrichment (Δ_v) depend on the temperature at the isotopic steady state. Thus, the $\delta^{18}O_{leaf}$ and δ^2H_{leaf} values were predicted to be associated primarily with temperature, RH, and source water, which is consistent with the results from the cluster analysis that the $\delta^{18}O_{leaf}$ and δ^2H_{leaf} values were clustered with temperature (MAT and MMT) and RH (MARH; Fig. 2b). Based on the C-G model, we plotted the measured and predicted $\delta^{18}O_{leaf}$ and δ^2H_{leaf} values (Fig. 3a, c) and observed no significant differences between the measured and predicted values of $\delta^{18}O_{leaf}$ and δ^2H_{leaf} values (Fig. 3b, d). This is because our threerepeated samplings occur during the day when leaf water is generally near an isotopic steady state because chloroplasts are mostly located near the evaporative sites (Cernusak et al., 2016). The non-steady state effects on leaf water isotopes were expected at night because of low stomatal conductance (Cernusak et al., 2005; Cuntz et al., 2002; Cernusak et al., 2016). Although the slopes of the predicted and measured $\delta^{18}O_{leaf}$ and $\delta^{2}H_{leaf}$ values were less than one, the C-G model still provides a reasonable framework for guiding the analysis of the different controls on $\delta^{18}O_{leaf}$ and $\delta^{2}H_{leaf}$ values.

4.2 Dual $\delta^{18}O$ and $\delta^{2}H$ plots of leaf water

There was a significant linear correlation between the $\delta^{18}O_{leaf}$ and $\delta^{2}H_{leaf}$ values, with remarkable clusters associated with the three months studied (Fig. 4). As is well-known, the LMWL, generated by precipitation $\delta^{18}O$ and $\delta^{2}H$ values at the local scale, serves as an important reference line for inter-comparisons among different waters. Furthermore, the regression lines of the $\delta^{18}O$ and $\delta^{2}H$ values from soil water, twig water, and leaf water (Supplementary Fig. S2) suggest that the leaf water isotopes could well inherit isotopic signals of source waters that originate from twig water, soil water, and ultimately precipitation. The slopes and intercepts of the $\delta^{18}O$ and $\delta^{2}H$ values decreased significantly from precipitation, soil water, twig water, and leaf water for each month, except for soil water in May (Supplementary Fig. S2). Such patterns have been observed in a number of previous calibration studies (Brooks et al., 2010; Evaristo et al., 2015; Sprenger et al., 2016, 2017; Wang et al., 2017; Benettin et al., 2018; Barbeta et al., 2019; Penna and Meerveld, 2019; Liu et al., 2021a). The slopes of the LMWLs were lower in July (6.79) relative to those from May (7.04) and September (6.85), but were not significantly different (ANCOVA test: df = 0.47, $F = 2.49$, $p = 0.11 > 0.05$). This suggests that the local water vapour from precipitation was derived from the same source across the seasons, but was subject to different intensities of evaporation as the temperature changed through the seasons (Li et al., 2019; Wu et al., 2019, 2021). The slopes of the $\delta^{18}O$ and $\delta^{2}H$ values from the soil, twig, and leaf waters were also much smaller than the LMWLs across the months due to the occurrence of secondary evaporation in the other water types.

In the dual isotope plot of leaf water, there were well-defined clusters of $\delta^{18}O_{leaf}$ and $\delta^{2}H_{leaf}$ values across the three months: ^{18}O and ^{2}H were depleted in September, there were intermediate values in July, and ^{18}O and ^{2}H were enriched in May (Fig. 4). When focusing on each month, relatively higher isotopic values occurred at low elevations, but lower isotopic values were present at high elevations despite there being no, or only weak, correlations between the $\delta^{18}O_{leaf}$ and $\delta^{2}H_{leaf}$ values and altitude (Supplementary Fig. S3). The correlations between the $\delta^{18}O_{leaf}$ and $\delta^{2}H_{leaf}$ values and altitude, and between the $\delta^{18}O_{twig}$ and $\delta^{2}H_{twig}$ values and altitude, were not significant and weak across the three months; however, the $\delta^{18}O_{p}$ and $\delta^{2}H_{p}$, and also the $\delta^{18}O_{soil}$ and $\delta^{2}H_{soil}$ values, were significantly correlated with altitude (Supplementary Fig. S3), which suggests that besides source water (precipitation and soil water), other factors associated with plants also affect the $\delta^{18}O_{leaf}$ and $\delta^{2}H_{leaf}$ values.

The dual isotope plot of $\delta^{18}O_{leaf}$ and $\delta^{2}H_{leaf}$ values show a significant isotope line: $y = 4.52x - 50.7$ ($R^2 = 0.81$, $p < 0.01$; Fig. 4), but relatively shallower slopes (3.53, 1.86, and 2.81 in May, July, and September, respectively) of $\delta^{18}O_{leaf}$ and $\delta^{2}H_{leaf}$ values were observed across the seasons (Supplementary Fig. S2). Such a correlation was supported by a recent study that conducted consecutive measurements of $\delta^{18}O$ and $\delta^{2}H$ values in xylem/leaf water in Switzerland and indicated that leaf water provided the great potential to determine the source water of plants (Benettin et al., 2021). Our local study showed remarkable clusters in the measured (Fig. 4) and the C-G model predicted (Fig. 3) $\delta^{18}O_{leaf}$ and $\delta^{2}H_{leaf}$ values across the months and the consistencies of respective $\delta^{18}O_{leaf}$ and $\delta^{2}H_{leaf}$ values with potential source water isotopes across months (Supplementary Fig. S1). These findings of temporally consistent dynamics among the water types (i.e., precipitation, soil water, twig/stem water, and leaf water) have been observed in a number of previous studies (Phillips and Ehleringer, 1995; Cernusak et al., 2005; Sprenger et al., 2016; Berry et al., 2017; Liu et al., 2021a).

The isotopic inheritance from precipitation to leaf water indicates that seasonal variations of $\delta^{18}O_{p}$ and $\delta^{2}H_{p}$ values are the first-order control on the temporal patterns seen in the leaf water. The seasonal dynamics of the $\delta^{18}O_{p}$ and $\delta^{2}H_{p}$ values reflect the combined effects of such things as temperature, altitude, and precipitation amount, which are associated with orographic conditions, as well as sub-cloud evaporation, moisture recycling, and differences in the vapor source (Dansgaard, 1964; McGuire and McDonnell, 2007; Li et al., 2016; Penna and Meerveld, 2019; Wu et al., 2019). In this study, we used the HYSPLIT model to demonstrate the ultimate cause of the seasonal variations of $\delta^{18}O_{leaf}$ and $\delta^{2}H_{leaf}$ values; that is, the monthly dynamics of the $\delta^{18}O_{p}$ and $\delta^{2}H_{p}$ values. The monthly variations of the $\delta^{18}O_{p}$ and $\delta^{2}H_{p}$ values from the Global Network for Isotopes in Precipitation (GNIP, http://www.iaea.org/) at Xi'an station (1985-1992 AD), which is ~100 km from our study transect, were enriched in ^{18}O and ^{2}H in May relative to July and September (Fig. 5a, b). The cluster mean of the moisture transport routes from HYSPLIT (Draxler and Rolph, 2003) and the climatological 850 hPa wind vectors showed that the main moisture sources were from western China and central Asia in May, the China-India Peninsula and Bay of Bengal, and local moisture recycling and convection (Fig. 5c, d, e). The seasonal variations in $\delta^{18}O_{p}$ and $\delta^{2}H_{p}$ values are consistently related to the onset, advancement, and retreat of the Asian summer monsoon and associated changes in the large-scale monsoon circulation (e.g., Zhang et al., 2020, 2021). As the summer monsoon starts in mid-May, the rainfall season starts in southern China; however, our study area is controlled mainly by moisture from the westerlies (Chiang et al., 2015) with relatively higher vapour, $\delta^{18}O_{p}$, and $\delta^{2}H_{p}$ values (Fig. 5c, a, b). In July, the summer monsoon reaches its strongest phase, and the rainfall belt shifts to central and northern China, where the southerly wind brings plenty of moisture from the China-India Peninsula and the Bay of Bengal with lower vapour, $\delta^{18}O_{p}$, and $\delta^{2}H_{p}$ values (Fig. 5d, a, b). When the summer monsoon withdraws in September, the study area is controlled mainly by local moisture recycling and convection (Fig. 5e). Soil water stores the June-August monsoon rainfall with its lower $\delta^{18}O$ and $\delta^{2}H$ values, resulting in even lower $\delta^{18}O_{p}$ and $\delta^{2}H_{p}$ values in September than in July (Supplementary Fig. S1), and thus resulting in significantly lower $\delta^{18}O$ and $\delta^{2}H$ values of leaf water (Fig. 4).

4.3 Framework of controls for $\delta^{18}O$ and $\delta^{2}H$ values of leaf water

To delineate the mechanisms that control the $\delta^{18}O_{leaf}$ and $\delta^{2}H_{leaf}$ values, we used the SEMs to quantify the complex interactions among $\delta^{18}O_{leaf}$ or $\delta^{2}H_{leaf}$ values, source waters, and meteorological parameters (Fig. 6). The coefficients of determination (R^2) were 0.48 and 0.71 for the $\delta^{18}O_{leaf}$ and $\delta^{2}H_{leaf}$ values, respectively, indicating that the models explained more variance for $\delta^{2}H_{leaf}$ values than $\delta^{18}O_{leaf}$ values (Fig. 6). The SEMs showed that potential source waters (i.e., twig water, soil water, and precipitation) had stronger effects on $\delta^{2}H_{leaf}$ relative to $\delta^{18}O_{leaf}$ values, while the meteorological parameters showed weak effects on both $\delta^{18}O_{leaf}$ and $\delta^{2}H_{leaf}$ values (a little larger for $\delta^{2}H_{leaf}$ than $\delta^{18}O_{leaf}$ values). This is consistent with our above correlation analysis (Fig. 2). Surprisingly, MMT had significant effects on $\delta^{18}O_{p}$ and $\delta^{2}H_{p}$ values, suggesting that temperature plays a key role in determining $\delta^{18}O_{p}$ and $\delta^{2}H_{p}$ values, but this finding is not discussed further here. Collectively, the SEMs also showed that source water exerts the first-order control but affects $\delta^{18}O_{leaf}$ and $\delta^{2}H_{leaf}$ differently; the meteorological parameters had a weak control on $\delta^{18}O_{leaf}$ and $\delta^{2}H_{leaf}$, with a more substantial effect on $\delta^{2}H_{leaf}$ than $\delta^{18}O_{leaf}$ values.

A schematic representation of the controls on $\delta^{18}O_{leaf}$ and $\delta^{2}H_{leaf}$ values (respective and dual) is shown in Fig. 7. It involves multiple processes associated with the hydroclimatic and biochemical factors that affect $\delta^{18}O_{leaf}$ and $\delta^{2}H_{leaf}$ values. The meteorological parameters (temperature, RH, and precipitation) exerted distinct effects on the $\delta^{18}O$ and $\delta^{2}H$ values of the source water, and thus on the $\delta^{18}O_{leaf}$ and $\delta^{2}H_{leaf}$ values, as demonstrated above by the SEM. Significant isotopic fractionation occurred mainly at two key locations across the vertical soil profiles and leaf architectures from precipitation to leaf water. First, an isotopic gradient across the vertical soil profile appeared because of evaporation from the surface soil layers (Ehleringer et al., 1992; Goldsmith et al., 2012; Evaristo et al., 2015). This evaporative isotopic fractionation causes an isotopic linear trajectory down the soil profile (Goldsmith et al., 2012; Rothfuss and Javaux, 2017; Wu et al., 2018; Wang et al., 2019; Amin et al., 2020; Zhao et al., 2020; Liu et al., 2021a). Second, there were significant isotopic heterogeneities because of transpiration associated with the $\delta^{18}O_{leaf}$ (Helliker and Ehleringer, 2000; Farquhar and Gan, 2003; Gan et al., 2003; Song et al., 2015) and $\delta^{2}H_{leaf}$ values (Šantrůček et al., 2007; Liu et al., 2016; Liu et al., 2021b) within a leaf, which depends substantially on veinal structures (Liu et al., 2021b). The within-leaf heterogeneity of the $\delta^{18}O_{leaf}$ and $\delta^{2}H_{leaf}$ values can be explained using the *Péclet*-modified C-G model (Gan et al., 2003; Farquhar and Gan, 2003; Cernusak et al., 2005, 2016). Collectively, the soil evaporation and leaf transpiration produce isotopic enrichment above source water (precipitation or soil water). Soil evaporation leads to an isotopic gradient across the vertical soil profile, providing water sources for plant roots uptake without isotope fractionation during the process (Dawson and Ehleringer, 1991; Ehleringer and Dawson, 1992; Chen et al., 2020). During the water transport between roots and leaf petioles, isotopic compositions of xylem water remain unaltered from that in soils (i.e. soil immobile water), until it reaches the leaf, which undergoes water loss (Ehleringer and Dawson, 1992). Within the leaf, transpiration leads to significant isotopic enrichment (Helliker and Ehleinger, 2000; Liu et al., 2015; Cernusak et al., 2016), which is highly dependent on meteorological parameters (e.g., temperature and relative humidity). However, the meteorological parameters (e.g., temperature, RH, precipitation, etc.) varied with altitude and seasonality, yielding an isotopic water line (LWL) in the dual-isotope plot (Fig. 4). The LWL generation provides an important baseline for leaf-derived organic matter such as cellulose (e.g., Barbour, 2007; Lehman et al., 2017) and leaf wax (Liu et al., 2016, 2021). Overall, the LWL is controlled primarily by altitude and seasonality, as these are the main influences on the hydroclimatic factors.

5 Conclusion

Along an elevation transect on the Chinese Loess Plateau, precipitation, soil water, twig water, and leaf water were repeatedly sampled to explore the controls on $\delta^{18}O_{leaf}$ and $\delta^{2}H_{leaf}$ values associated with meteorological parameters and source water. The effects of meteorological parameters and source water on $\delta^{18}O_{leaf}$ and $\delta^{2}H_{leaf}$ values were different, and the dual $\delta^{18}O_{leaf}$ and $\delta^{2}H_{leaf}$ plot generated an isotopic line. We found that $\delta^{2}H_{leaf}$ values were more closely correlated with source water isotopes than $\delta^{18}O_{leaf}$ values, whereas $\delta^{18}O_{leaf}$ and $\delta^{2}H_{leaf}$ values were similarly correlated with meteorological parameters. The observations suggest that plant organic isotopic proxies such as leaf wax and cellulose originating from $\delta^{18}O_{leaf}$ and $\delta^{2}H_{leaf}$ values can provide comparative climatic information. Additionally, the dual-isotope analysis showed that the $\delta^{18}O_{leaf}$ and $\delta^{2}H_{leaf}$ values were closely correlated because of their similar altitudinal and seasonal responses. The first-order control on $\delta^{18}O_{leaf}$ and $\delta^{2}H_{leaf}$ values was the source water (i.e., precipitation), and the meteorological parameters had a comparative effect on both $\delta^{18}O_{leaf}$ and $\delta^{2}H_{leaf}$ values, which varied with altitude and season. In the future, we will investigate the relationship of an intersection angle θ with the hydroclimatic and biochemical factors.

Competing interests

The authors declare that they have no known competing financial interests or personal relationships that could have appeared to influence the work reported in this paper.

Acknowledgement

We thank X. Cao and M. Xing for help with laboratory assistance, and Y. Cheng for the help in the field. We thank Profs. J. J. McDonnell and L. A. Cernusak for discussing and editing the paper. We also thank Shaanxi Meteorological Bureau for supporting meteorological data along an elevation transect. This work was supported by the Chinese Academy of Sciences (XDB40000000; XAB2019B02; ZDBS-LY-DQC033; 132B61KYSB20170005) and the National Natural Science Foundation of China (42073017).

Author contribution

J.L. conceived the idea of research, and performed the data analysis. J.L., H.W., and H.Z. wrote the manuscript. L.G. and Y.Z. edited the paper. J.L. and C.J. performed the lab work. All authors contributed to discuss the results.

Data availability statement

Data related to this article can be found in Electric Annex and Mendeley Data (https://data.mendeley.com/drafts/t44wybgpr3).

References

Amin, A., Zuecco, G., Geris, J., Schwendenmann, L., McDonnell, J.J., Borga, M., and Penna, D.: Depth distribution of soil water sourced by plants at the global scale: a new direct inference approach, Ecohydrology, 13, e2177, 2020.

Allison, G., Barnes, C., and Hughes, M.: The distribution of deuterium and ^{18}O in dry soils 2. Experimental, J. Hydrol., 64, 377–397, 1983.

Barbeta, A., Jones, S. P., Clavé, L., Gimeno, T. E., Fréjaville, B., Wohl, S., and Ogée, J.: Unexplained hydrogen isotope offsets complicate the identification and quantification of tree water sources in a riparian forest, Hydrol. Earth Syst. Sci., 23, 2129–2146, 2019.

Barbour, M. M.: Stable oxygen isotope composition of plant tissue: a review. Funct. Plant Biol., 34, 83–94, 2007.

Barbour, M. M., Farquhar, G. D., and Buckley, T. N.: Leaf water stable isotopes and water transport outside the xylem, Plant Cell Environ., 40, 914–920, 2017.

Benettin, P., Nehemy, M. F., Cernusak, L. A., Kahmen, A., and McDonnell, J. J.: On the use of leaf water to determine plant water source: A proof of concept, Hydrol. Process., DOI: 10.1002/hyp.14073, 2021.

Benettin, P., Volkmann, T. H. M., von Freyberg, J., Frentress, J., Penna, D., Dawson, T. E., and Kirchner, J. W.: Effects of climatic seasonality on the isotopic composition of evaporating soil waters, Hydrol. Earth Syst. Sci., 22, 2881–2890, 2018.

Berry, Z. C., Evaristo, J., Moore, G., Poca, M., Steppe, K., Verrot, L., Asbjornsen, H., Borma, L. S., Bretfeld, M., Herve-Fernandez, P., Seyfried, M., Schwendenmann, L., Sinacore, K., Wispelaere, L. D., and McDonnell, J.: The two water worlds hypothesis: addressing multiple working hypotheses and proposing a way forward, Ecohydrology, e1843, 2017.

Bottinga, Y., and Craig., H.: Oxygen isotope fractionation between CO_2 and water, and the isotopic composition of marine atmospheric CO_2, Earth Planet. Sci. Lett., 5, 285–295, 1969.

Bowen, G. J., and Revenaugh, J.: Interpolating the isotopic composition of modern meteoric precipitation, Water Resour. Res., 39, 1299, 2003.

Bowen, G. J.: Isoscapes: Spatial pattern in isotopic biogeochemistry, Annu. Rev. Earth Planet. Sci., 2010, 161–187, 2010.

Bowen, G. J., and Good, S. P.: Incorporating water isoscapes in hydrological and water resource investigations, Wiley Interdiscip. Rev. Water, 2, 107–119, 2015.

Brooks, J. R., Barnard, H. R., Coulombe, R., and McDonnell, J. J.: Ecohydrologic separation of water between trees and streams in a Mediterranean climate, Nat. Geosci., 3, 100–104. 2010.

Cernusak, L. A., Farquhar, G. D., and Pate, J. S.: Environmental and physiological controls over oxygen and carbon isotope composition of Tasmanian blue gum, *Eucalyptus globulus*, Tree Physiol., 25, 129–146, 2005.

Cernusak, L. A., Barbour, M. M., Arndt, S. K., Cheesman, A. W., English, N. B., field, T. S., Helliker, B. R., Holloway-Phillips, M. M., Holtum, J. A. M., Kahmen, A., McInerney, F. A., Munksgaard, N. C., Simonin, K. A., Song, X., Stuart-Williams, H., West, J. B., and Farquhar, G. D.: Stable isotopes in leaf water of terrestrial plants. Plant Cell Environ., 39, 1087–1102, 2016.

Cernusak, L. A., Barbeta, A., Bush, R., Eichstaedt R., Ferrio, J., Flanagan, L., Gessler, A., Martín-Gómez, P., Hirl, R., Kahmen, A., Keitel., C., Lai, C., Munksgaard, N., Nelson, D., Ogée J., Roden, J., Schnyder, H., Voelker, S., Wang L., Stuart-Williams, H., Wingate, L., Yu, W., Zhao, L., Cuntz, M., 2022. Do ^{2}H and ^{18}O in leaf water reflect environmental drivers differently? New Phytologist, DOI: 10.1111/nph.18113.

Chen. Y., Helliker, B. R., Tang, X., Li, F., Zhou, Y., and Song, X.: Stem water cryogenic extraction biases estimation in deuterium isotope composition of plant source water, Proc. Natl. Acad. Sci., 117, 33345–33350, 2020.

Chiang, J. C., Fung, I. Y., Wu, C. -H., Cai, Y., Edman, J. P., Liu, Y., Day, J. A., Bhattacharya, T., Mondal, Y., and Labrousse, C. A.: Role of seasonal transitions and westerly jets in East Asian paleoclimate, Quat. Sci. Rev., 108, 111–129, 2015.

Craig, H., and Gordon, L. I.: Deuterium and oxygen-18 variations in the ocean and the marine atmosphere. In ‘Proceedings of a conference on stable isotopes in oceanographic studies and paleotemperatures', pp. 9–130, 1965.

Cuntz M., Ogée J., Farquhar G.D., Peylin P. & Cernusak L.A.: Modelling advection and diffusion of water isotopologues in leaves. Plant Cell Environ. 30, 892–909, 2007.

Dansgaard, W.: Stable isotopes in precipitation, Tellus, 16, 436–468, 1964.

Dawson, T. E. and Ehleringer, J. R.: Streamside trees that do not use stream water, Nature, 350, 335–337, 1991.

Dongmann. G., Nurnberg, H. E., Forstel, H., and Wagener, K.: On the enrichment of $H_2^{18}O$ in the leaves of transpiring plants, Radiat. Environ. Biophys. 11, 41–52, 1974.

Draxler, R. R., and Rolph, G. D.: HYSPLIT (Hybrid Single-Particle Lagrangian Integrated Trajectory) Model Access via NOAA ARLREADY. htmlNOAA Air Resources Laboratory, http://www.arl.noaa.gov/ready/hysplit4, 2003.

Ehleringer, J. R. and Dawson, T. E: Water uptake by plants: perspectives from stable isotope composition, Plant Cell Environ., 15, 1073–1082, 1992.

Ehleringer, J. R. and Dawson, T. E.: Water uptake by plants: perspectives from stable isotope composition, Plant Cell Environ., 15, 1073–1082, 1992.

Ellsworth, P. Z., and Williams, D. G.: Hydrogen isotope fractionation during water uptake by woody xerophytes, Plant Soil, 291, 93–107, 2007.

Evaristo J., Jasechko S., and McDonnell J. J.: Global separation of plant transpiration from groundwater and streamflow, Nature, 525, 91–94, 2015.

Farquhar, G. D., Cernusak, L. A., and Barnes, B.: Heavy water fractionation during transpiration, Plant Physiol., 143, 11–18, 2007.

Farquhar, G. D., and Cernusak, L. A.: On the isotopic composition of leaf water in the non- steady state, Funct. Plant Biol., 32, 293–303, 2005.

Farquhar, G..D., and Gan, K..S.: On the progressive enrichment of the oxygen isotopic composition of water along leaves, Plant Cell Environ., 26, 801–819, 2003.

Farquhar, G. D., and Lloyd, J.: Carbon and oxygen isotope effects in the exchange of carbon dioxide between terrestrial plants and the atmosphere. In Stable Isotopes and Plant Carbon–Water Relations (eds J.R. Ehleringer, A.E. Hall, & G.D. Farquhar), pp. 47–70. Academic Press, San Diego, 1993.

Gan, K.S., Wong, S.C., Yong, J.W.H., Farquhar, G.D., 2003. Evaluation of models of leaf water^{18}O enrichments of spatial patterns of vein xylem, leaf water and dry matter in maize leaves. Plant Cell Environ. 26, 1479–1495.

Goldsmith, G. R., Munoz-Villers, L. E., Holwerda, F., McDonnell, J. J., Asbjornsen, H., and Dawson, T. E.: Stable isotopes reveal linkages among ecohydrological processes in a seasonally dry tropical montane cloud forest, Ecohydrology, 5, 779–790, 2012.

Helliker, B. R., and Ehleringer, J. R.: Establishing a grassland signature in veins: ^{18}O in the leaf water of C_3 and C_4 grasses, Proc. Natl. Acad. Sci., 97, 7894–7898, 2000.

Hepp, J., Schäfer, I. K., Lanny, V., Franke, J., Blidtner, M., Rozanski, K., Glaser, B., Zech, M., Eglinton, T. I., and Zech, R.: Evaluation of bacterial glycerol dialkyl glycerol tetraether and ^{2}H-^{18}O biomarker proxies along a central European topsoil transect, Biogeosciences, 17, 741–756, 2020.

Kahmen, A., Sachse, D., Arndt, S. K., Tu, K. P., Farrington, H., Vitousek, P. M., and Dawson, T. E.: Cellulose δ^{18}O is an index of leaf-to-air vapor pressure difference (VPD) in tropical plants, Proc. Natl. Acad. Sci., 108, 1981–1986, 2011.

Leaney, F., Osmond, C., Allison, G., and Ziegler, H.: Hydrogen-isotope composition of leaf water in C_3 and C_4 plants: its relationship to the hydrogen-isotope composition of dry matter, Planta, 164, 215–220, 1985.

Lehmann, M. M., Gamarra, B., Kahmen, A., Siegwolf, R. T. W., and Saurer, M.: Oxygen isotope fractionations across individual leaf carbohydrates in grass and tree species. Plant Cell Environ., 40, 1658–1670, 2017.

Li, Z., Feng, Q., Wang, Q., Kong, Y., Cheng, A., Yong, S., Li, Y., Li, J., and Guo, X.: Contributions of local terrestrial evaporation and transpiration to precipitation using $\delta^{18}O$ and D-excess as a proxy in Shiyang inland river basin in China, Global Planet. Change, 146, 140–151, 2016.

Li, Z., Li, Z., Yu, H., Song, L., and Ma, J.: Environmental significance and zonal characteristics of stable isotope of atmospheric precipitation in arid Central Asia. Atmos. Res., 227, 24–40, 2019.

Lin, G. H., and Sternberg, L. S. L.: Hydrogen isotopic fractionation by plant roots during water uptake in coastal wetland plants. Stable Isotopic and Plant Carbon/Water Relations, Academic Press, New York, pp. 497–510, 1993.

Liu, J., Liu, W., and An, Z.: Insight into the reasons of leaf wax $\delta D_{n\text{-alkane}}$ values between grasses and woods, Sci. Bull., 60, 549–555, 2015.

Liu, J., Liu, W., An, Z., and Yang, H.: Different hydrogen isotope fractionations during lipid formation in higher plants: Implications for paleohydrology, Sci. Report, 6, 19711, 2016.

Liu, J., Wu, H., Cheng, Y., Jin, Z., and Hu, J.: Stable isotope analysis of soil and plant water in a pair of natural grassland and understory of planted forestland on the Chinese Loess Plateau, Agr. Water Manage., 249, 106800, 2021a.

Liu, J., An, Z., and Lin, G.: Intra-leaf heterogeneities of hydrogen isotope compositions in leaf water and leaf wax of monocots and dicots, Sci. Total Environ., 770, 145258, 2021b.

Liu, J.: Seasonality of the altitude effect on leaf wax n-alkane distributions, hydrogen and carbon isotopes along an arid transect in the Qinling Mountains. Sci. Total Environ., 778, 146272, 2021.

Majoube M. Fractionnement en oxygen-18 et en deuterium entre l’eau et sa vapeur. Journal de Chimie et Physique 68, 1423–1436, 1971.

McGuire, K., and McDonnell J. J.: Stable isotope tracers in watershed hydrology, in Stable Isotopes in Ecology and Environmental Science, Ecological Methods and Concepts Series, pp. 334–374, 2007.

Munksgaard, N. C., Cheesman, A. W., English, N. B., Zwart, C., Kahmen, A., and Cernusak, L. A.: Identifying drivers of leaf water and cellulose stable isotope enrichment in Eucalyptus in northern Australia, Oecologia, 183, 31–43, 2017.

Ogée, J., Cuntz, M., Peylin, P., Bariac, T., 2007. Non-steady-state, non-uniform transpiration rate and leaf anatomy effects on the progressive stable isotope enrichment of leaf water along monocot leaves. Plant Cell Environ. 30, 367–387.

Pagani, M., Pedentchouk, N., Huber, M., Sluijs, A., Schouten, S., Brinkhuis, H., Damsté, J. S. S., and Dichens, G. R.: Arctic hydrology during global warming at the Palaeocene/Eocene thermal maximum, Nature, 442, 671–675, 2006.

Penna, D., and van Meerveld, H. J.: Spatial variability in the isotopic composition of water in small catchments and its effect on hydrograph separation, WIREs Water, e1367, 2019.

Phillips, S. L., and Ehleringer, J. R.: Limited uptake of summer precipitation by big tooth maple (*Acer grandidentatum* Nutt) and Gambels oak (*Quercus gambelii* Nutt), Trees, 9, 214–219, 1995.

Plavcová, L., Hronková, M., Šimková, M., Květoň, J., Vráblová, M., Kubásek, J., Šantrůček, J.: Seasonal variation of $\delta^{18}O$ and $\delta^{2}H$ in leaf water of *Fagus sylvatica* L. and related water compartments, J. Plant Physiol., 227, 56–65, 2018.

Poca, M., Coomans, O., Urcelay, C., Zeballos, S. R., Bodé, S., and Boecks, P.: Isotope fractionation during root water uptake by *Acacia caven* is enhanced by arbuscular mycorrhizas, Plant Soil, 441, 485–497, 2019.

Romero, I.C., Feakins, S.I., 2011. Spatial gradients in plant leaf wax D/H across a coastal salt marsh in southern California. Org. Geochem. 42, 618–629.

Rothfuss, Y., and Javaux, M.: Reviews and syntheses: isotopic approaches to quantify root water uptake: a review and comparison of methods, Biogeosciences, 14, 2199–2224, 2017.

Sachse, D., Billault, I., Bowen, G.J., Chikaraishi, Y., Dawson, T.E., Feakins, S.J., Freeman, K.H., Magill, C.R., McInerney, F.A., van der Meer, M.T.J., Polissar, P.J., Robins, R.J., Sachs, J.P., Schmidt, H.L., Sessions, A.L., White, J.W.C., West, J.B., Kahmen, A., 2012. Molecular paleoyhydrology: interpreting the hydrogen-isotopic composition of lipid biomarkers from photosynthesizing organisms. Annu. Rev. Earth

Planet. Sci. 40, 221–249.

Šantrůček, J., Květoň, J., Šetlík, J., Bulíčková, L., 2007. Spatial variation of deuterium enrichment in bulk water of snowgun leaves. Plant Physiol. 143, 88–97.

Song, X., Loucos, K. E., Simonin, K. A., Farquhar, G. D., and Barbour, M. M.: Measurements of transpiration isotopologues and leaf water to assess enrichment models in cotton, New Phytol., 206, 637–646, 2015.

Schefuβ, E., Kuhlmann, H., Mollenhauer, G., Prange, M., and Pätzold, J.: Forcing of wet phases in Southeast Africa over the past 17,000 year, Nature, 480, 22–29, 2011.

Sprenger, M., Leistert, H., Gimbel, K., and Weiler, M.: Illuminating hydrological processes at the soil-vegetation-atmosphere interface with water stable isotopes, Rev. Geophys., 54, 674–704, 2016.

Sprenger, M., Tetzlaff, D., and Soulsby, S.: Soil water stable isotopes reveal evaporation dynamics at the soil-plant-atmosphere interface of the critical zone, Hydrol. Earth Syst. Sci., 21, 3839–3858, 2017.

Wang, J., Fu, B., Lu, N., and Zhang, L.: Seasonal variation in water uptake patterns of three plant species based on stable isotopes in the semi-arid Loess Plateau, Sci. Total Environ., 609, 27–37, 2017.

Wang, J., Lu, N., and Fu, B.: Inter-comparison of stable isotope mixing models for determining plant water source partitioning, Sci. Total Environ. 666, 685–693, 2019b.

Wu, H., Li, J., Li, X., He, B., Liu, J., Jiang, Z., and Zhang, C.: Contrasting response of coexisting plant's water-use patterns to experimental precipitation manipulation in an alpine grassland community of Qinghai Lake watershed, China, PLoS One, 13, e0194242, 2018.

Wu, H., Wu, J., Sakiev, K., Liu, J., Li, J., He, B., Liu, Y., and Shen, B.: Spatial and temporal variability of stable isotopes ($\delta^{18}O$ and $\delta^{2}H$) in surface waters of arid, mountainous Central Asia, Hydrol. Process. 33, 1658–1669, 2019.

Wu, H., Huang, Q., Fu, C., Song, F., Liu, J., Li, J.: Stable isotope signatures of river and lake water from Poyang Lake, China: Implications for river-lake interactions. J. Hydrol. 592, 125619, 2021.

Zhang, P., and Liu, W.: Effect of plant life form on relationship between δD values of leaf wax *n*-alkanes and altitude along Mount Taibai, China, Org. Geochem., 42, 100–107, 2010.

Zhao, L., Wang, L., Cernusak, L. A., Liu, X., Xiao, H., Zhou, M., and Zhang, S.: Significant difference in hydrogen isotope composition between xylem and tissue water in *Populus Euphratica*, Plant Cell Environ., 39, 1848–1857, 2016.

Zhao, Y., Wang, Y., He, M., Tong, Y., Zhou, J., Guo, X., Liu, J., Zhang, X.: Transference of *Robinia pseudoacacia* water-use patterns from deep to shallow soil layers during the transition period between the dry and rainy seasons in a waterlimited region, For. Ecol. Manag., 457, 117727, 2020.

Zhang, H., Cheng, H., Cai, Y., Spötl, C., Sinha, A., Kathayat, G., Li, H.: Effect of precipitation seasonality on annual oxygen isotopic composition in the area of spring persistent rain in southeastern China and its paleoclimatic implication, Clim. Past, 16, 211–225, 2020.

Zhang, H., Zhang, X., Cai, Y., Sinha, A., Spötl, C., Baker, J., Kathayat, G., Liu, Z., Tian, Y., and Lu, J.: A data-model comparison pinpoints Holocene spatiotemporal pattern of East Asian summer monsoon, Quat. Sci. Rev., 261, 106911, 2021.

Figure captions

Fig. 1 Sample sites (red dots) and weather stations (open triangles) that distribute along vertical vegetation zones across the Mt. Taibai transect on the Chinese Loess Plateau (a). The meteorological parameters (precipitation, temperature, and RH) vary with stations along elevation transect (b). Mean annul (MAP, MAT, MARH) and montly (MMP, MMT, MMRH) precipitation, temperature, and relative humidity. The subscripts refer to the month. The vertical vegetation distribution was adopted from Liu, 2021.

Fig. 2 Heatmaps of correlations (*r*) between leaf water $\delta^{18}O$ and $\delta^{2}H$ values and potential source water $\delta^{18}O$ and $\delta^{2}H$ values (twig water, soil water, and precipitation $\delta^{18}O$ and $\delta^{2}H$ values; a), and meteorological parameters (e.g., MAP, MMP, MAT, MMT, MARH, MMRH). The hierarchical cluster analysis of the isotopes of leaf water and source water (a), and meteorologica parameters (b). The subscripts (p, soil, twig, leaf) refer to precipitation, soil water, twig water, and leaf water. * Corrected significance at $p < 0.05$; ** corrected significance at $p < 0.01$; *** corrected significance at $p < 0.001$.

Fig. 3 Measured leaf water isotopic composition for $\delta^{18}O$ (a) and $\delta^{2}H$ (c) values against values predicted by the C-G model. Boxplots show no significant differences for $\delta^{18}O$ (b) and $\delta^{2}H$ (d) values between measured and predicted leaf water. The dotted lines show one-to-one lines.

Fig. 4 Correlation of leaf water $\delta^{18}O$ and $\delta^{2}H$ values across months and altitude. Leaf water $\delta^{18}O$ and $\delta^{2}H$ values were the higher in May, intermediate in July, and lower in September, and while within each month, those isotopic values were relatively lower at high altitudes and higher in lower altitudes.

Fig. 5 Variation of monthly mean precipitation $\delta^{18}O$ (a) and $\delta^{2}H$ (b) values at Xi'an station from Global Network of Isotopes in Precipitation (GNIP) and cluster mean of moisture transport routes using HYSPLIT model in May (c), July (d) and September (e), 2020. Background in (c-e) is the average precipitation (mm/day) and 850 hPa wind vectors (arrows, m/s) in May (c), July (d) and September (e) in 1979-2016 AD based on the database of the Global Precipitation Climatology Center (GPCC) (Becker et al., 2011) and the Modern-Era Retrospective analysis for Research and Applications (Rienecker et al., 2011).

Fig. 6 Structural equation model (SEM) of leaf water $\delta^{18}O$ (a) and $\delta^{2}H$ (b) values. The structural equation models considered all plausible pathways. Solid lines indicate significant positive (red) or negative (blue) effects, and dashed lines indicate non-significant effects. Grey lines indicate correlations between two variables. Numbers on the arrow indicate significant standardized path coefficients, proportional to the arrow width. The coefficients of determination (R^2) represent the proportion of variance explained by the model.

Fig. 7 Schematics of the respective and dual isotopes of $\delta^{18}O$ and $\delta^{2}H$ values from precipitation to leaf water, associated with physical (evaporation at soil profile and transpiration at leaf level) and biochemical processes. The dual isotopes of $\delta^{18}O$ and $\delta^{2}H$ values yield an isotopic water line, the slope of which was lower than the LMWL. The intersected angle varied with hydroclimates, associated with altitude and seasonality.

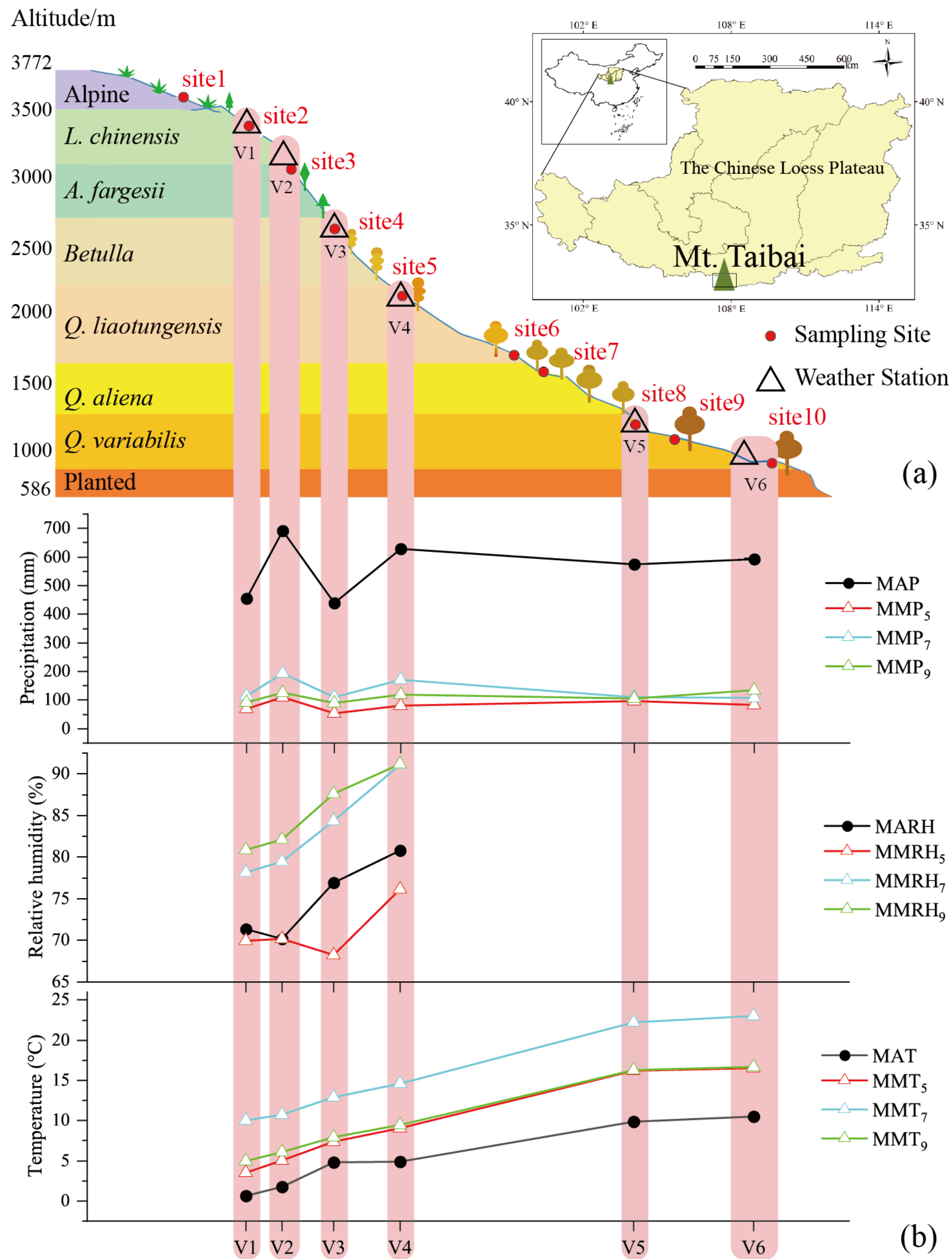

Altitude/m
3772
3500
3000
2500
2000
1500
1000
586
Alpine
L. chinensis
A. fargesii
Betulla
Q. liaotungensis
Q. aliena
Q. variabilis
Planted
site1
site2
site3
site4
site5
site6
site7
site8
site9
site10
V1
V2
V3
V4
V5
V6
The Chinese Loess Plateau
Mt. Taibai
Sampling Site
Weather Station
(a)
Precipitation (mm)
MAP
MMP5
MMP7
MMP9
Relative humidity (%)
MARH
MMRH5
MMRH7
MMRH9
Temperature (°C)
MAT
MMT5
MMT7
MMT9
(b)

Figure-1

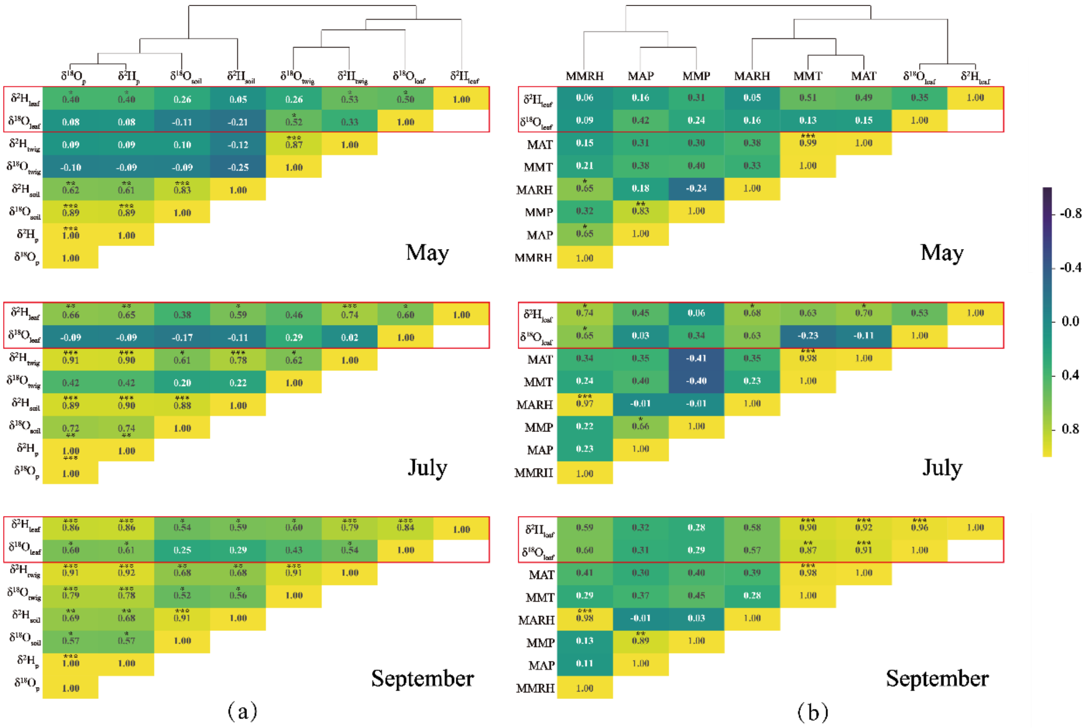

Figure-2

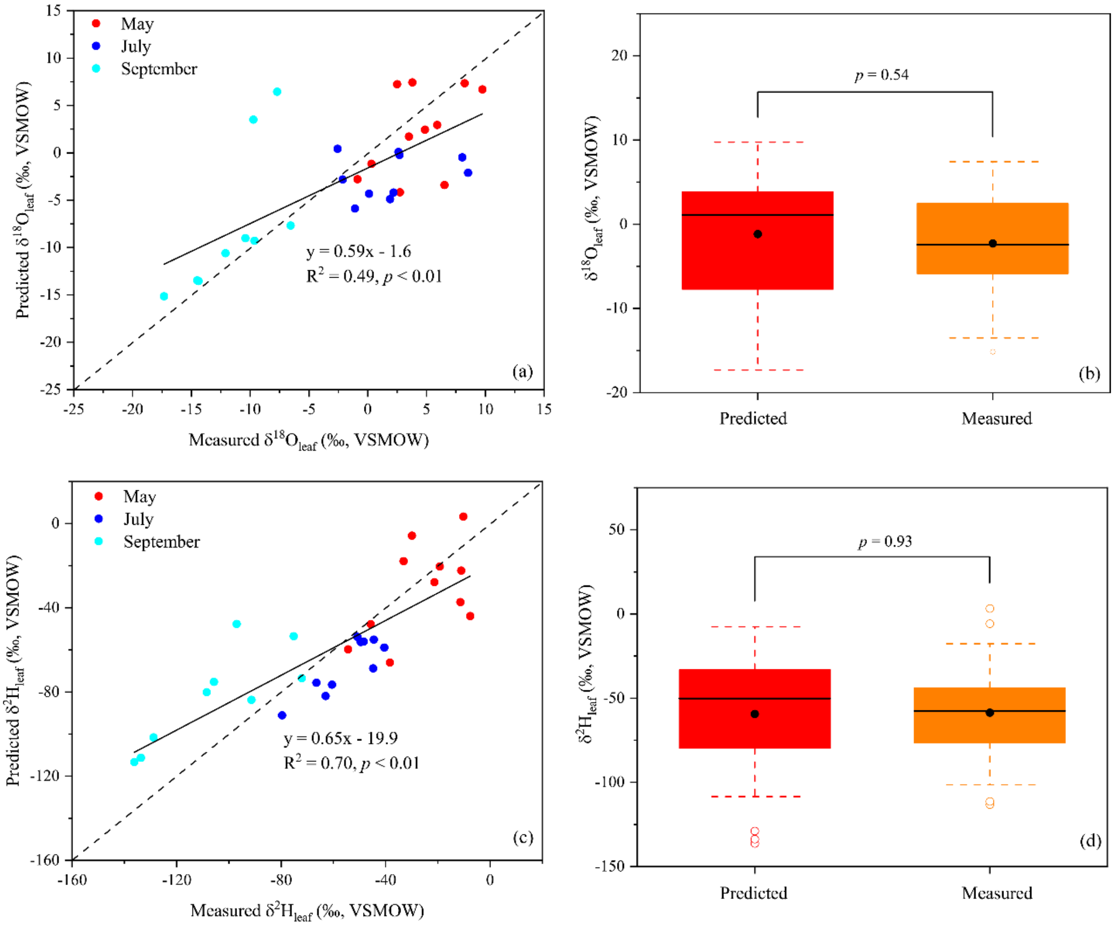

May
July
September
y = 0.59x - 1.6
R2 = 0.49, p < 0.01
(a)
Predicted δ18Oleaf (‰, VSMOW)
Measured δ18Oleaf (‰, VSMOW)
p = 0.54
(b)
δ18Oleaf (‰, VSMOW)
Predicted
Measured
May
July
September
y = 0.65x - 19.9
R2 = 0.70, p < 0.01
(c)
Predicted δ2Hleaf (‰, VSMOW)
Measured δ2Hleaf (‰, VSMOW)
p = 0.93
(d)
δ2Hleaf (‰, VSMOW)
Predicted
Measured

Figure-3

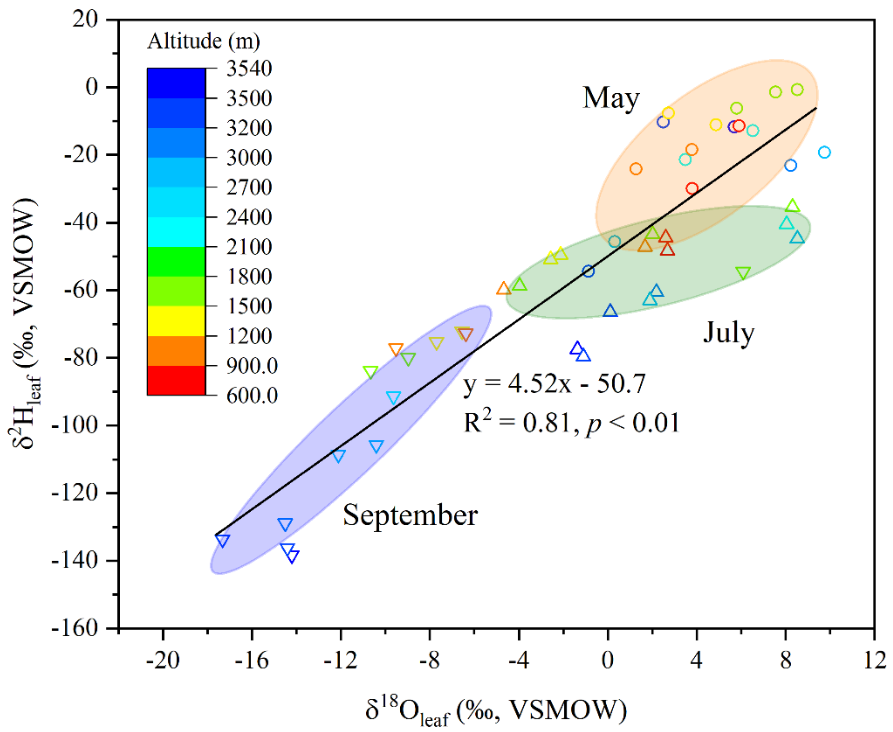

Figure-4

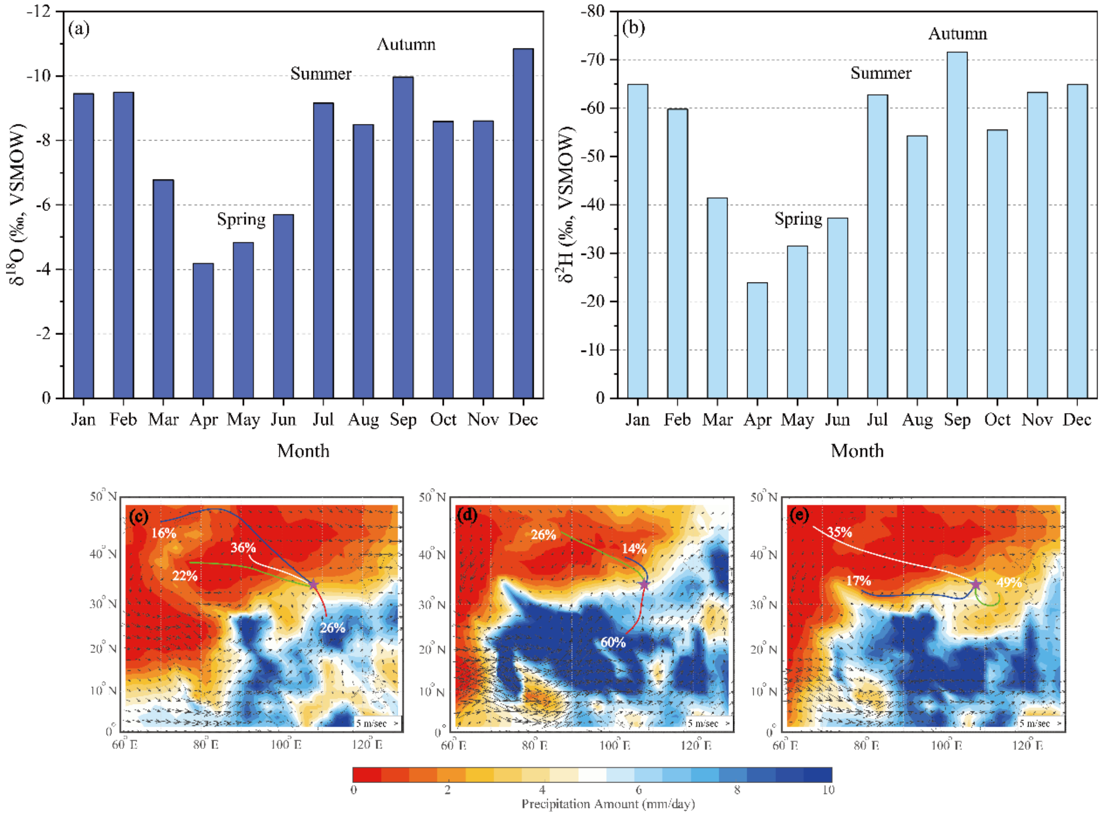

Figure-5

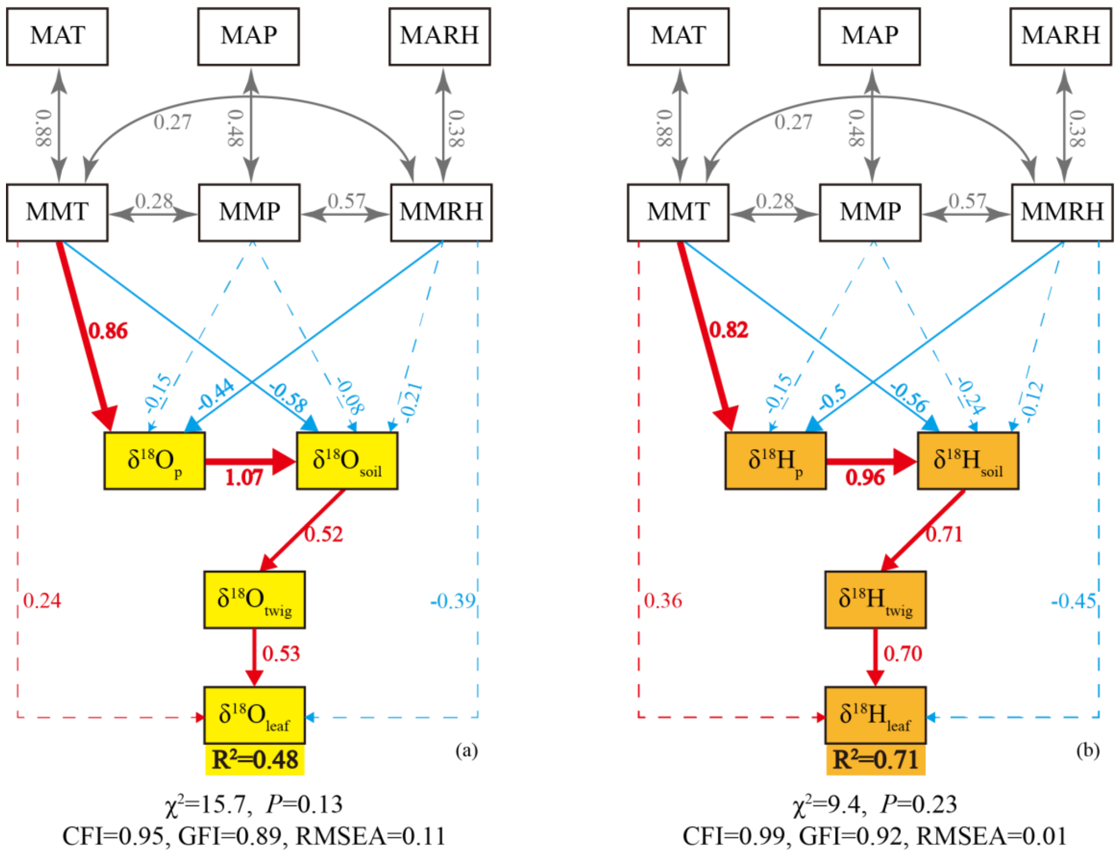

Figure-6

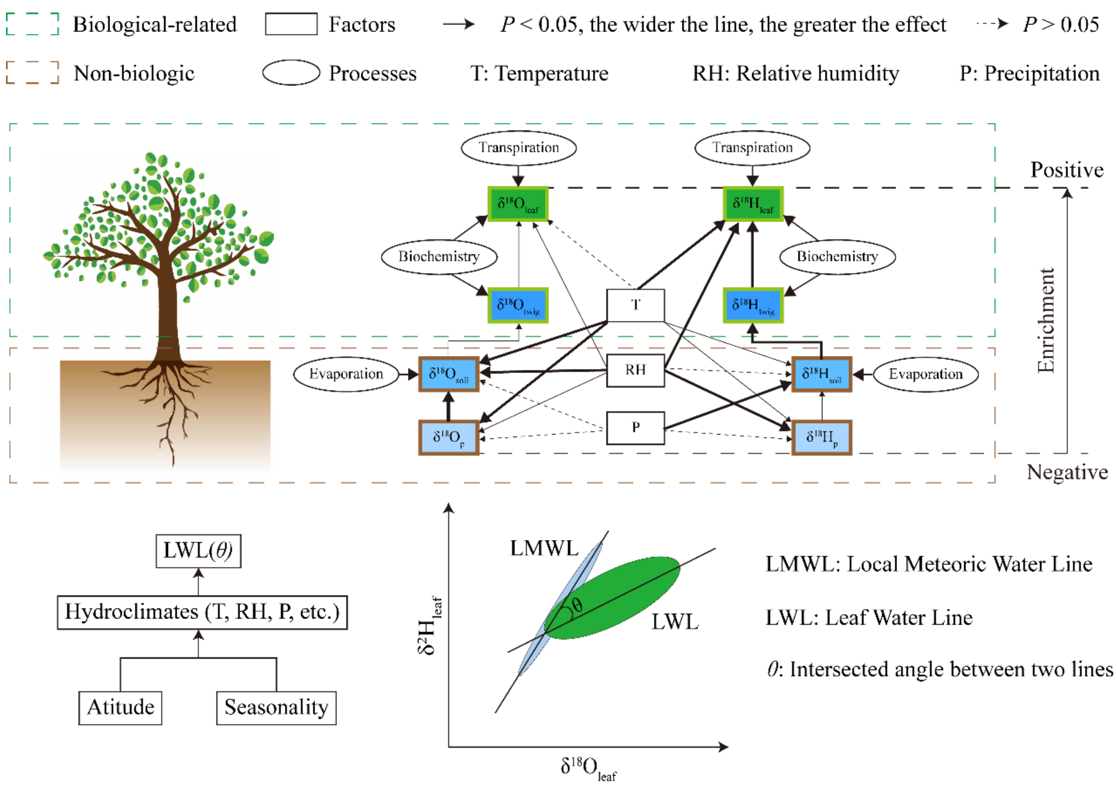

Figure-7